学位論文

Development of the Gene Therapy with a CRE Decoy ODN to Prevent Vascular Intimal Hyperplasia

（CRE decoy ODNを用いた血管内膜肥厚抑制遺伝子治療）

旭川医科大学大学院医学系研究科博士課程医学専攻

内田　大貴

（齊藤　幸裕、菊地　信介、吉田　有里、平田　哲、
笹嶋　唯博、東　信良と共著）

Development of gene therapy with a cyclic adenosine monophosphate response element decoy oligodeoxynucleotide to prevent vascular intimal hyperplasia

Daiki Uchida, MD, Yukihiro Saito, MD, PhD, Shinsuke Kikuchi, MD, PhD, Yuri Yoshida, MD, Satoshi Hirata, MD, PhD, Tadahiro Sasajima, MD, PhD, *and* Nobuyoshi Azuma, MD, PhD, *Asahikawa, Hokkaido, Japan*

ABSTRACT

Objective: Intimal hyperplasia (IH) is the main cause of therapeutic failure after vascular and endovascular surgery. However, there is currently no targeted therapy for the treatment of IH. We recently reported that the inhibition of cyclic adenosine monophosphate response element (CRE) binding protein (CREB) activation is important in vein graft IH. We focused on a decoy oligodeoxynucleotide (ODN) therapeutic strategy for suppressing IH as a clinical application. The objective of this study was to confirm the therapeutic effect of a *CRE* decoy ODN in an animal model as a novel therapy for preventing intimal hyperplasia as the first step of the preclinical study of our strategy.

Methods: We designed two phosphorothioate *CREs* and two scramble decoy ODNs and screened them using a CREB transcription assay to check their ability to bind to a CRE sequence. We chose a *CRE* decoy ODN with high first-binding ability and transfected it into vascular smooth muscle cells (VSMCs) in vitro. Proliferation and migration were assessed using MTS (3-(4,5-dimethylthiazol-2-yl)-5-(3-carboxymethoxyphenyl)-2-(4-sulfophenyl)-2H-tetrazolium) assays and modified Boyden chamber assays. We examined *CRE* activity using a luciferase reporter gene assay. We assessed the expression of messenger RNAs by quantitative real-time polymerase chain reaction. In a wire-injury mouse model (C57BL6, n = 6), *CRE* decoy ODN was transfected into the injured vessel wall using an ultrasound-sonoporation method in vivo. Mitogen-activated protein kinase-activated protein kinase 3 (*MAPKAPK3*) and four and a half LIM domains 5 (*FHL5*) expression of pregrafting vein remnants were assessed by immunohistologic analyses.

Results: Compared with scramble decoy ODN, the selected *CRE* decoy ODN could significantly decrease *CRE* activity (mean ± standard error of the mean: 0.20 ± 0.03 vs 1.00 ± 0.16, n = 6; $P < .05$) as shown by a luciferase reporter gene assay, VSMC proliferation (0.73 ± 0.04 vs 0.89 ± 0.02, n = 6; $P < .05$) and migration (96.4 ± 6.1 vs 311.4 ± 19.1 migrated VSMCs/well, n = 6; $P < .05$) after 24-hour transfection. The *CRE* decoy ODN significantly suppressed the formation of IH at injured vessel walls in an animal model, as analyzed by pathologic staining (0.20 ± 0.02 vs 0.56 ± 0.08, area of the intima/area of the artery vs the control after 21 days' transfection, n = 6; $P < .05$). Furthermore, MAPKAPK3 and FHL5, which are CREB activators, were significantly expressed in pregrafting vein remnants in diabetes mellitus patients.

Conclusions: CREB-CRE signaling is an important mechanism of IH formation, and *CRE* decoy therapy can help preventing IH. This study is the first part of the preclinical study of our strategy. (J Vasc Surg 2019;■:1-13.)

Clinical Relevance: Intimal hyperplasia (IH) is an important topic of vascular and endovascular surgery with artery and vein in common. However, there is essentially nothing to prevent IH from occurring. The novel strategy using a cyclic adenosine monophosphate response element decoy oligodeoxynucleotide will provide new feasibility for controlling IH after vascular and endovascular surgery.

Keywords: CRE; Decoy; Gene therapy; Intimal hyperplasia

Intimal hyperplasia (IH) is an important postsurgical complication of vascular and endovascular surgery that affects arteries and veins, such as after bypass surgery using autologous vein grafts and restenosis after endovascular repair. Restenosis develops in 5.8% of patients undergoing carotid endarterectomy or receiving carotid stents.[1] Approximately 30% to 50% of limb vein grafts fail within 3 to 5 years,[2-4] and 60% of artery-venous shunts for hemodialysis access fail to mature.[5]

To improve these outcomes, few IH preventative strategies and therapies have been developed, including clinical drugs and devices. Although numerous potential

From the Division of Vascular Surgery, Department of Surgery, Asahikawa Medical University.

This work was partially supported by a Grants-in-Aid for Scientific Research (KAKENHI).

Author conflict of interest: none.

Correspondence: Yukihiro Saito, MD, PhD, Department of Surgery, Asahikawa Medical University, 2-1 Midorigaoka-Higashi, Asahikawa, Hokkaido 078-8510, Japan (e-mail: ys02067@asahikawa-med.ac.jp).

The editors and reviewers of this article have no relevant financial relationships to disclose per the JVS policy that requires reviewers to decline review of any manuscript for which they may have a conflict of interest.

0741-5214

https://doi.org/10.1016/j.jvs.2019.02.042

targeted experimental molecules for IH treatment have been successful in animal models, few strategies have been adopted for clinical use in patients.[6] For example, the Limus family of immunosuppressive agents was used in the treatment of coronary artery lesions via sirolimus-coated stents, but the resulting data regarding the rate of death or myocardial infarction were inconclusive with regard to efficacy.[7,8] An E2 factor (*E2F*) decoy was expected to be effective for the treatment of IH ex vivo, but late-phase clinical trials resulted in no significant improvement in graft patency in coronary or peripheral vein grafts.[9,10]

Furthermore, the evidence underlying these few approaches is frequently limited. The slow progress of basic science and clinical translation in this area is caused by (1) the low reproducibility of IH pathophysiology in cell culture and animal models, (2) the lack of a powerful live imaging system for minute vessels in vivo, and (3) the complexity of the IH process in humans, including background factors such as age, sex, complications, and medications.

In 2005, Mitra et al[11] reviewed the pathophysiological changes in vein walls during vein graft neointima formation and ordered these changes into the following five sequential steps: (1) platelet activation and correlated events, (2) inflammation with leukocyte recruitment, (3) activation of the coagulation cascade, and (4) vascular smooth muscle cell (VSMC) migration and (5) proliferation. Many researchers have tried to control these steps with molecules such as nuclear factor-κB (NF-κB),[12,13] matrix metalloproteinases (MMPs),[14-17] transforming growth factor-β,[18,19] interleukins,[20] growth factors,[21] and transcription factors.[22-24] Some authors have emphasized the importance of controlling VSMCs.

We recently identified two novel therapeutic genes, mitogen-activated protein kinase-activated protein kinase 3 (*MAPKAPK3*) and four and a half LIM domains 5 (*FHL5*) for controlling VSMCs by screening a human vein graft sample.[25] Briefly, *MAPKAPK3* and *FHL5* are highly expressed in human vein graft samples when analyzed by microarray. These molecules promote VSMC proliferation and migration. The messenger RNA expression of these genes is induced by stress conditions in VSMCs. MAPKAPK3 and FHL5 are both coactivators of the cyclic adenosine monophosphate response element (CRE) binding protein (CREB) family of transcription factors. We confirmed that both genes can activate CREB, but the mechanism of activation is different. Furthermore, we showed that dominant-negative CREB decreased cellular proliferation and migration and repressed the transcription of CREB-induced genes. In a wire-injury mouse model, the transfer of dominant-negative CREB suppressed IH.

Some reports have indicated a relationship between IH formation and CREB activity.[26,27] However, they focused solely on CREB phosphorylation, not on alternative pathways, or direct activation. There appear to be no reports to date on the clinical use of CREB phosphorylation. Our study investigated how CREB was activated by MAPKAPK3 and FHL5 by independent mechanisms. MAPKAPK3 activates CREB by phosphorylation of the Ser-133 site, and FHL5 activates CREB by direct binding, possibly to the kinase-inducible domain. In terms of therapeutic strategies for IH, inhibition of the phosphorylation of the Ser-133 site alone would not inhibit IH, and a more radical strategy is required to repress CREB function. We hypothesized that the *CRE* decoy ODN could be a novel therapeutic molecule for IH formation, because *CRE* decoy ODN acts as an inhibitor of activated CREB to bind CRE, regardless of the CREB activation pathway via MAPKAPK3 or FHL5.

Considering clinical data, diabetes mellitus (DM) and maintenance hemodialysis (HD) are widely considered to be major risk factors of ischemic heart disease and peripheral artery disease (PAD). Indeed, >60% of patients with PAD at our hospital had DM or HD, or both. Patients with DM have been reported to have an increased risk of restenosis after conventional stent implantation.[28] We believe that it should be determined whether CREB activators, MAPKAPK3 or FHL5, or both, are related to the high risk of restenosis in patients with DM and HD.

We plan to develop our "CREB preventative strategy" for IH suppression (Fig 1, *A*). Considering its translation to clinical use, *CRE* decoy therapy appears to be suitable for our strategy based on evidence from previous research.[9] The objective of this study was to confirm the therapeutic effect of a *CRE* decoy in an animal model as a novel therapy for preventing IH and to determine whether a *CRE* decoy is a candidate molecule for preventing IH. The present study is therefore regarded as the first step of the preclinical study of our strategy.

ARTICLE HIGHLIGHTS

- **Type of Research:** Experimental study using human vascular smooth muscle cells and a wire-injury mouse model
- **Key Findings:** The cyclic adenosine monophosphate response element (CRE) decoy oligodeoxynucleotide could significantly decrease *CRE* activity and vascular smooth muscle cell proliferation and migration. The *CRE* decoy oligodeoxynucleotide significantly suppressed the formation of IH at injured vessel walls in an animal model.
- **Take Home Message:** CRE binding protein-CRE signaling is an important mechanism in IH formation, and *CRE* decoy therapy can help to prevent IH.

METHODS

***CRE* decoy.** The phosphorothioate ODN sequences are provided in the Table. Each ODN was designed according to previous reports[29-31] and synthesized by

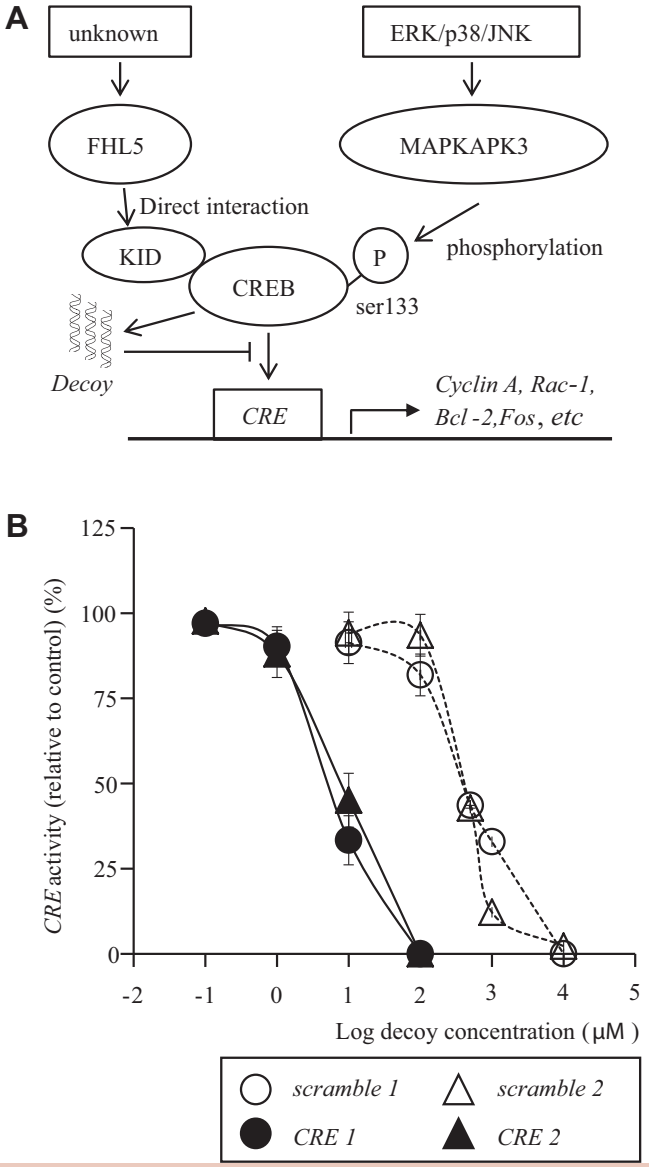

Fig 1. Functional screening of candidate cyclic adenosine monophosphate response element *CRE*) decoy oligodeoxynucleotide (ODN) and scramble decoy ODN. **A,** Schematic diagram of the CRE signaling pathways and our strategy using a *CRE* decoy ODN. **B,** *CRE* activity with *CRE* decoy ODN or scramble decoy ODN, as determined by a CRE binding protein (*CREB1*; phospho S133) Transcription Factor Assay Kit (n = 6). Half maximal inhibitory concentration: *CRE* decoy ODN (candidate 1) 7.814 pmol/μL and scramble decoy ODN (candidate 2) 3726.416 pmol/μL. Data are presented as the mean and standard error of the mean (*range bars*). *ERK,* Extracellular signal-regulated kinase; *JNK,* Jun NH_2-terminal kinase; *KID,* kinase-inducible domain; *FHL5,* four and a half LIM domains 5; *MAPKAPK3,* mitogen-activated protein kinase-activated protein kinase 3.

GeneDesign, Inc (Osaka, Japan). We prepared the *CRE* decoy ODN as functional molecules and the scramble decoy ODN as nonfunctional negative control molecules. *CRE* decoy ODNs conjugated with biotin and nonconjugated *CRE* decoy ODNs were prepared.

Table. The sequences of candidate decoy oligodeoxynucleotides

Candidate name	Sequences
CRE 1	5′-tgagccgctgacgtttacactcat-3′
CRE 2	5′-agagattgcctgacgtcagagagctag-3′
Scramble 1	5′-taagccaccagcagttacaatcat-3′
Scramble 2	5′-ggagtgaccaggtgttacaatcat-3′

CRE, Cyclic adenosine monophosphate response element.

Decoy activity assay. To evaluate the potential inhibition of *CRE* activity, each decoy ODN was checked using a CREB1 (phospho-S133) Transcription Factor Assay Kit (Abnova Corp, Taipei City, Taiwan) according to the manufacturer's protocol. This assay can evaluate the potential inhibition of *CRE* activity, because activated CREB is trapped by *CRE* decoy ODN when the *CRE* decoy ODN is added to the assay well, and CREB cannot bind to a well-coated *CRE* sequence.

Cell culture. Aortic SMCs were purchased (Lonza Walkersville Inc, Ford Road, Md) and maintained in smooth muscle growth medium (Lonza) supplemented with 10% fetal bovine serum and smooth muscle growth supplement (including recombinant human endothelial growth factor, insulin, GA-1000, human fetal growth factor, and bovine serum albumin). Cultures were incubated at 37°C in a humidified atmosphere of 95% air and 5% CO_2, with an exchange of medium every 2 days. These cells were used at passages 5 to 8 for the subsequent experimental protocols. Cells were transfected using Lipofectamine LTX (Thermo Fisher Scientific Inc, Fremont, Calif).

Immunofluorescent, immunohistologic, and pathologic analyses. Cells grown on glass coverslips or 4-μm frozen tissues sections were fixed in acetone for 5 minutes. The samples were permeabilized with 0.2% Triton X-100 in phosphate-buffered saline for 2 minutes. The samples were blocked in 5% skim milk and stained with streptavidin conjugated with Alexa Fluor 555 (Thermo Fisher Scientific). Then, 4-μm paraffin-embedded sections of human pregrafting vein remnants or mouse femoral artery samples were deparaffinized and rehydrated.

Mouse femoral artery samples were stained with hematoxylin and eosin (HE), Masson-Trichrome (MT), and elastica van Gieson (EVG).

Human pregrafting vein remnants were treated with buffer (pH 9.0; Nichirei Biosciences Inc, Tokyo, Japan) for antigen retrieval as described in the manufacturer's protocol. Samples were blocked in methanol with 3% H_2O_2 and stained with primary antibodies, including polyclonal rabbit anti-MAPKAPK3 and polyclonal rabbit anti-FHL5 (both Novus Biologicals, Littleton, Colo), for 1 hour at room temperature. The samples were stained using Histofine Max-PO and 3,3′-diaminobenzidine (Nichirei Biosciences).

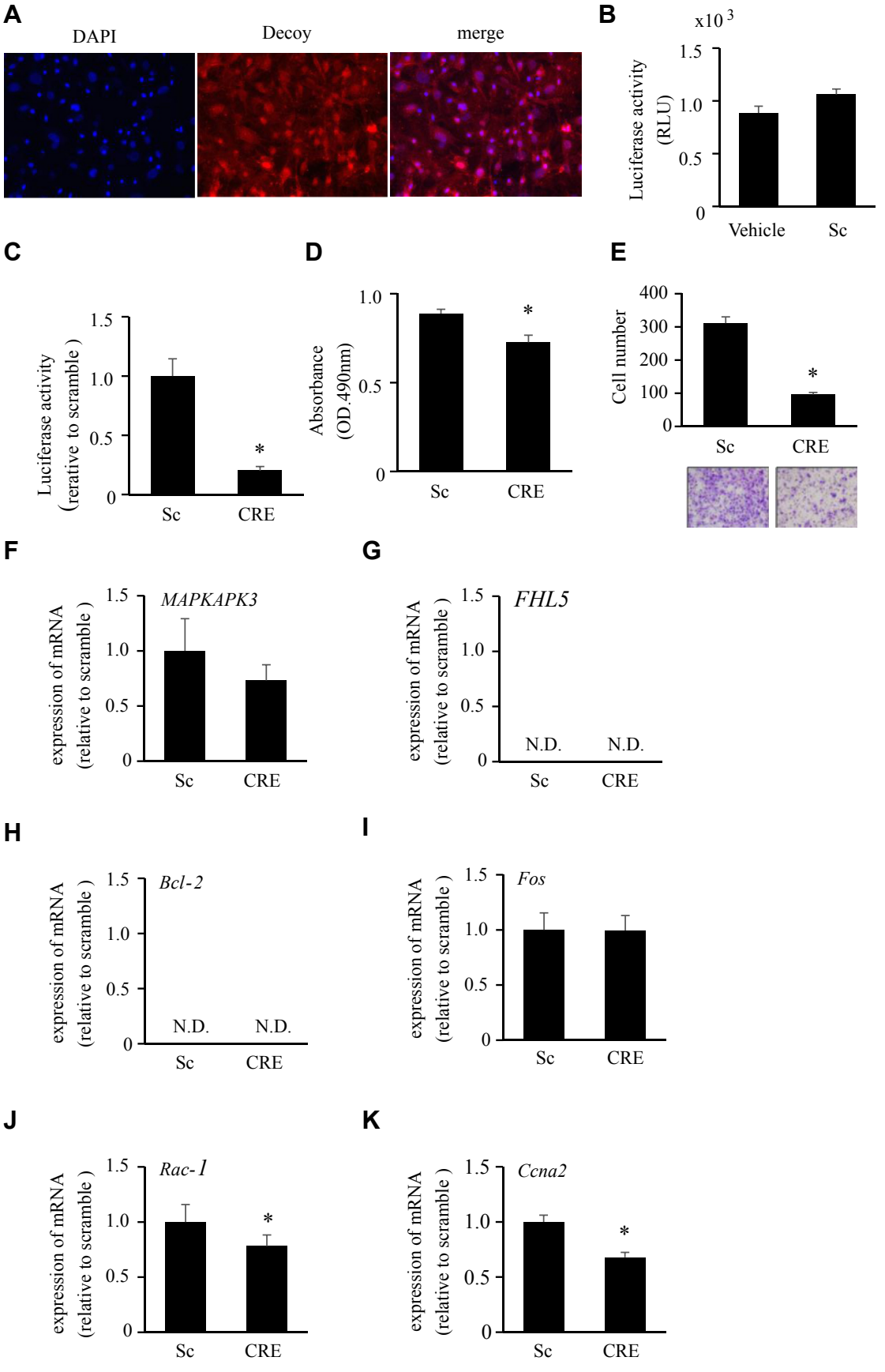
A
DAPI
Decoy
merge
B
x10 3
Luciferase activity (RLU)
1.5
1.0
0.5
0
Vehicle
Sc
C
Luciferase activity (rerative to scramble)
1.5
1.0
0.5
0
*
Sc
CRE
D
Absorbance (OD 490nm)
1.0
0.5
0
*
Sc
CRE
E
Cell number
400
300
200
100
0
*
Sc
CRE
F
MAPKAPK3
expression of mRNA (relative to scramble)
1.5
1.0
0.5
0
Sc
CRE
G
FHL5
expression of mRNA (relative to scramble)
1.5
1.0
0.5
0
N.D.
N.D.
Sc
CRE
H
Bcl-2
expression of mRNA (relative to scramble)
1.5
1.0
0.5
0
N.D.
N.D.
Sc
CRE
I
Fos
expression of mRNA (relative to scramble)
1.5
1.0
0.5
0
Sc
CRE
J
Rac-1
expression of mRNA (relative to scramble)
1.5
1.0
0.5
0
*
Sc
CRE
K
Ccna2
expression of mRNA (relative to scramble)
1.5
1.0
0.5
0
*
Sc
CRE

Luciferase reporter gene assay. VSMCs were cultured in 12-well dishes and transiently cotransfected with *CRE* decoy ODNs or scramble ODNs and a *CRE* reporter vector that contained a specific *cis*-acting DNA sequence (enhancer element) and a sensitive reporter gene (Pathway Profiling Luciferase System; Clontech Laboratories, Inc, Mountain View, Calif), as described in the manufacturer's protocol. This plasmid contained the luciferase reporter gene downstream of several copies of specific transcription factor-binding *CRE* sequences. After 24 hours, luciferase activity was determined using a Luciferase Assay System (Promega, Madison, Wisc).

Cell proliferation. The cell proliferation of VSMCs seeded in 12-well plates was measured with the MTS (3-(4,5-dimethylthiazol-2-yl)-5-(3-carboxymethoxyphenyl)-2-(4-sulfophenyl)-2H-tetrazolium) assay 24 hours after transfection with plasmid vectors. Approximately 200 μL of CellTiter 96 One Solution Reagent (Promega) in 1000 μL of Dulbecco's modified Eagle's medium was added to each well, and the absorbance was measured at 490 nm.

Cell migration. The migration of transfected VSMCs was estimated in a modified Boyden chamber. Cell migration was examined in a 48-well microchemotaxis chamber with polyvinyl pyrrolidone-free polycarbonate membranes (Neuro Probe Inc, Gaithersburg, Md) with 8-μm pores. Next, 32 μL of Dulbecco's modified Eagle's medium containing 10% fetal bovine serum was placed in the lower chamber. The membrane was positioned above the lower chamber, and 3×10^6 cells/mL were suspended in 50 μL of Dulbecco's modified Eagle's medium and added to the upper chamber. The Boyden chamber was incubated at 37°C for 24 hours. After incubation, the membrane was removed, and the cells on the upper side of the membrane were scraped off. The cells on the lower side of the membrane were stained with Diff-Quick (Sysmex, Hyogo, Japan), and the cells were counted in five randomly chosen fields under original magnification ×200.

Real-time quantitative polymerase chain reaction. Total RNA was extracted with RNeasy Plus Mini (Qiagen, KJ Venlo, Netherlands). Complementary DNA was synthesized with the Transcriptor High Fidelity cDNA Synthesis Kit (Roche Diagnostics, Mannheim, Germany). Relative gene copy numbers of target genes and *β-actin* were quantified by real-time reverse transcriptase polymerase chain reaction with TaqMan Gene Expression Assays (*Mapkapk3*, Mm00628676; *Fh15*, Mm00480451; *Ccna2*, Mm00438064; *Fos*, Mm00487425; *Rac1*, Mm01201657; *Bc12*, Mm00477631; *actin β*, Mm00607939; *MAPKAPK3*, Hs00177957; *FHL5*, Hs00220910; *CCNA2*, Hs00996788; *FOS*, Hs00170630; *RAC1*, Hs01902432; *BCL2*, Hs00608023; and *ACTIN β*, 99999903; Applied Biosystems, Foster City, Calif). The absolute number of gene copies was normalized to *β-actin* and standardized by a sample standard curve.

Mouse wire-injury model and gene transfer protocol. All animal protocols were approved by the Asahikawa Medical College Animal Ethics Committee. Wild-type male C57BL/6J mice (11 weeks old) were anesthetized with 1.5% to 2.5% isoflurane in a mixture of air. Surgery was performed as described previously.[32] The left femoral artery was exposed by blunt dissection. The accompanying femoral nerve was carefully separated, but the femoral vein was not isolated from the artery. The femoral artery and vein were looped at proximal and distal sites with 6-0 silk sutures for temporary vascular control during the procedure. A small branch between the rectus femoris and vastus medialis muscles was isolated, looped proximally, and ligated distally with 6-0 silk sutures. Veins and connective tissues around the artery were carefully removed. The exposed muscular branch artery was dilated by the topical application of one drop of 1% lidocaine hydrochloride. A transverse arteriotomy was performed in the muscular branch.

A straight spring wire (0.38 mm in diameter, No. C-SF-15-15; Cook, Bloomington, Ind) was carefully inserted into the femoral artery >5 mm toward the iliac artery. The wire was left in place for 1 minute to denude and dilate the artery. Then, the wire was removed. The injured segment was transiently isolated by temporary ligatures.

Fig 2. Function and mechanism of cyclic adenosine monophosphate response element (*CRE*) decoy oligodeoxynucleotide (ODN) in vitro. **A,** Representative images of *CRE* decoy ODN conjugated with biotin transfected into vascular smooth muscle cells (VSMCs). The transfection efficiency was >70%, calculated by the number of biotin-positive cells/4′,6-diamidino-2-phenylindole (*DAPI*)-positive cells. **B,** Effect of transfection regent (vehicle alone) compared with vehicle as nonfunctional control (scramble [*Sc*] decoy ODN; n = 4). **C,** Effect of *CRE* decoy ODN on VSMCs luciferase transcription, which is driven by the *CRE* motif, as determined by reporter gene assay (n = 6). *$P < .05$ vs scramble decoy ODN (Sc). Effect of candidate gene plasmid on VSMCs **(D)** proliferation as determined by MTS (3-(4,5-dimethylthiazol-2-yl)-5-(3-carboxymethoxyphenyl)-2-(4-sulfophenyl)-2H-tetrazolium) assays and **(E)** migration as determined by Boyden chamber assays (n = 6). *$P < .05$ vs scramble decoy ODN. Gene expression of **(F)** mitogen-activated protein kinase-activated protein kinase 3 (*MAPKAPK3*) and **(G)** four and a half LIM domains 5 (*FHL5*) in VSMCs after transfection with *CRE* decoy ODN (n = 12). Expression of genes downstream of the *CRE* element, including **(H)** *Bcl-2*, **(I)** *Fos*, **(J)** *Rac-1*, and **(K)** *Ccna2*, after 24-hour transfection with the *CRE* decoy ODN (n = 12). *$P < .05$ vs scramble decoy ODN. Data are presented as mean and standard error of the mean (*range bars*). *mRNA,* Messenger RNA; *N.D.,* not detected; *OD,* optical density; *RLU,* relative light units.

The *CRE* decoy ODN or scramble decoy ODN was transfected using a microbubble-enhanced ultrasound method. A silicon tube (0.40 mm in diameter) was cannulated in the same hole of the muscle branch artery. The decoy with 30% SV-25 microbubble solution (NepaGene, Chiba, Japan) was infused into the femoral artery through the silicon tube and incubated within the lumen with ultrasound for 10 seconds (2.5 W/cm^2).

Femoral arteries were collected 5 days after injury for gene expression analysis and at 21 days after injury for pathologic analysis. For pathologic analysis, cross-sections were stained with the HE, MT, and EVG methods. Morphometric analysis was performed using the image analysis software ImageJ (National Institutes of Health, Bethesda, Md), and the following values were calculated: artery area, lumen ratio (area of lumen/area of artery), intima ratio (area of intima/area of artery), media ratio (area of media/area of artery), and adventitia ratio (area of adventitia/area of artery).

Human pregrafting vein remnants. The operations for the study patients were performed between January 2002 and December 2011 at Asahikawa Medical University Hospital. The patients were diagnosed with arteriosclerosis obliterans and required surgical treatment. All patients provided written informed consent. The study protocol was approved by the Asahikawa Medical University Institutional Review Board and conformed to the Declaration of Helsinki tenets and the Japanese Ministerial Ordinance.

The harvested veins used for bypass surgery as grafts were classified as good, fair, and poor during the operation by the surgeon before grafting, according to our assessment criteria: caliber, distensibility, findings of phlebosclerosis, inflammation, and varicose changes.[33] The pregrafting autologous vein remnants were obtained at surgery for further examination.

Statistical analysis. Data were compared using the unpaired Student *t*-test for comparisons between two groups, analysis of variance followed by the Dunnett test for pairwise comparisons against the control, and the Tukey test for multiple comparisons. Differences were considered significant at $P < .05$.

RESULTS

Screening of candidate *CRE* and scramble decoy ODNs. The candidate *CRE* decoy ODN and scramble decoy ODN were designed as shown in the Table. On the basis of the results from the decoy activity assay, *CRE* candidate 1 and scramble candidate 2 were used (Fig 1, *B*). Using an approximation, the half maximal inhibitory concentration values were calculated, with 7.814 pmol/μL for the *CRE* decoy ODN (candidate 1) and 3726.416 pmol/μL for the scramble decoy ODN (candidate 2). Therefore, the *CRE* decoy ODN could inhibit *CRE* activity 476 times better than the scramble decoy ODN.

We also confirmed the molecular mechanism to suppress *CRE* activity using the *CRE* decoy ODN because the decoy activity assay could detect the binding of CREB to CRE, which was immobilized in the wells of a 96-well plate, or the *CRE* decoy ODN using a nonradioactive, sensitive method. We thus confirmed that the *CRE* decoy ODN could bind to activated CREB directly and effectively inhibit CREB from binding to the *CRE* element by the addition of the *CRE* decoy ODN into the wells.

Function and effect of *CRE* decoy ODN in vitro. Immunofluorescent staining demonstrated that the transfection efficiency of the *CRE* decoy ODN was >70%, and the *CRE* decoy ODN was localized mainly in the nucleus of VSMCs (Fig 2, *A*). Our transfection method had no impact on CRE activity (Fig 2, *B*).

To confirm the function of the *CRE* decoy ODN, *CRE* activity was assessed in VSMCs using a luciferase reporter gene assay. The *CRE* decoy ODN significantly inhibited *CRE* activity compared with the scramble decoy ODN ($P < .05$; Fig 2, *C*). Furthermore, the proliferation and migration of VSMCs transfected with the *CRE* decoy ODN or scramble decoy ODN were assessed. Transfer of the *CRE* decoy ODN significantly decreased VSMC proliferation and migration compared with the scramble decoy ODN ($P < .05$; Fig 2, *D* and *E*).

We next focused on *MAPKAPK3* and *FHL5* expression in the VSMCs. Transfer of the *CRE* decoy ODN did not significantly affect *MAPAPK3* expression compared with the scramble decoy ODN (Fig 2, *F*). In contrast, *FHL5* expression was not detected in the *CRE* decoy ODN or scramble decoy ODN transfer (Fig 2, *G*).

We also examined the expression of genes downstream of the *CRE* element, including *Bcl-2*, *Fos*, *Rac-1*, and *Ccna2*. *Bcl-2* expression was not detected regardless of whether the *CRE* decoy ODN or scramble decoy ODN was transferred into the VSMCs (Fig 2, *H*). Transfer of the *CRE* decoy ODN did not affect *Fos* expression compared with the scramble decoy ODN (Fig 2, *I*). However, *Rac-1* and *Ccna2* expression were suppressed by transfer of the *CRE* decoy ODN compared with transfer of the scramble decoy ODN (Fig 2, *J* and *K*).

Gene transfer into the vascular wall in vivo. Given the in vitro data, we aimed to reveal the gene therapy effect of the *CRE* decoy ODN for IH suppression in an animal model. A wire-injury mouse model was created, and the *CRE* decoy ODN or scramble decoy ODN was transfected into the injured artery using an ultrasound-sonoporation method. This mouse model has been used in many previous studies as an IH model in general. We confirmed a high transfection efficiency to the vascular wall with the *CRE* decoy ODN conjugated with biotin via immunofluorescent staining (Fig 3, *A*).

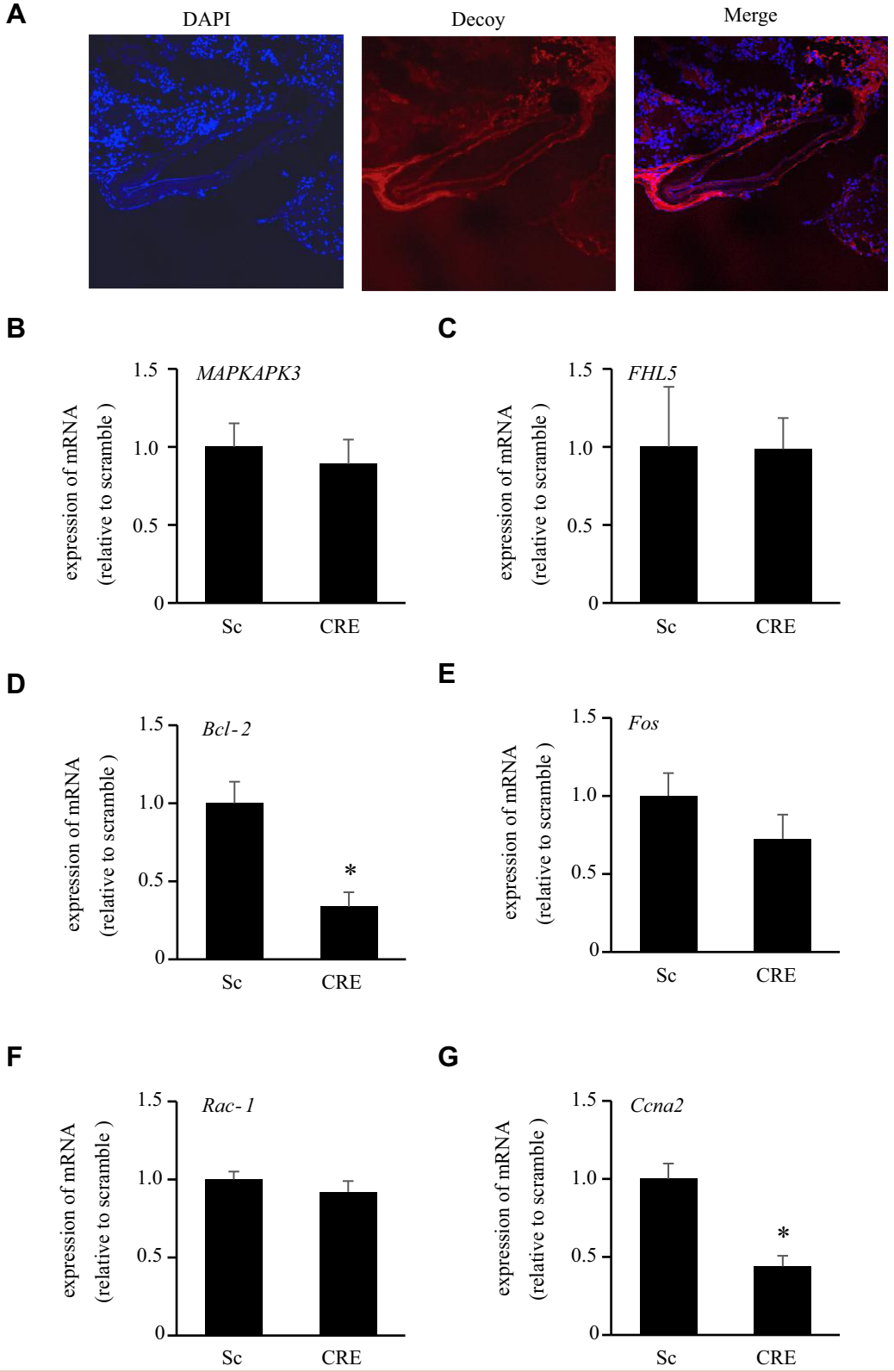

Fig 3. Transfer and effect of cyclic adenosine monophosphate response element (*CRE*) decoy oligodeoxynucleotide (ODN) in vivo. **A,** Representative images of *CRE* decoy ODN conjugated with biotin transfected into the vascular wall in vivo. The decoy was detected not only in the intima but also in the media and adventitia. The transfection efficiency was >80%, as calculated by the biotin-positive area/4′,6-diamidino-2-phenylindole (*DAPI*)-positive area. Gene expression of **(B)** mitogen-activated protein kinase-activated protein kinase 3 (*MAPKAPK3*) and **(C)** four and a half LIM domains 5 (*FHL5*) in the vascular wall after 21 days of transfection with the *CRE* decoy ODN (n = 6). Expression of genes downstream of the *CRE* element, including **(D)** *Bcl-2* (D), **(E)** *Fos*, **(F)** *Rac-1*, and **(G)** *Ccna2*, after 21 days of transfection with the *CRE* decoy ODN (n = 6). *$P < .05$ v. scramble (*Sc*) decoy ODN. *mRNA*, Messenger RNA.

Gene expression was assessed in whole-vessel samples transfected with the *CRE* decoy ODN or scramble decoy ODN at 5 days after surgery by real-time quantitative polymerase chain reaction. We initially focused on the expression of *MAPKAPK3* and *FHL5*, because these molecules are activators of CREB. Neither gene was affected by the transfer of the *CRE* decoy ODN or scramble decoy ODN (Fig 3, *B* and *C*). Surprisingly, *FHL5* was detected in whole-vessel samples even though it was not detected in VSMCs.

We next determined the expression of *Bcl-2*, *Fos*, *Rac-1*, and *Ccna2* in whole-vessel samples as well as in VSMCs. *Bcl-2* expression was detected in the whole-vessel samples and was significantly suppressed by the *CRE* decoy ODN compared with the expression observed after application of the scramble decoy ODN (Fig 3, *D*). The *CRE* decoy ODN did not affect *Fos* and *Rac-1* expression compared with the scramble decoy ODN (Fig 3, *E* and *F*). *Ccna2* expression was significantly suppressed by the *CRE* decoy ODN compared with the scramble decoy ODN (Fig 3, *G*).

These results differ from those observed in the VSMCs with respect to *FHL5*, *Bc12*, and *Rac-1* expression.

Gene therapy with *CRE* decoy ODN in vivo. Histopathologic analysis showed that the wire-treated arteries, for both the scramble and *CRE* decoy groups, were dilated by the wire treatment compared with the control group artery, which was not treated by the wire (Fig 4, *A*). Indeed, the artery area from the scramble and *CRE* groups was significantly increased compared with that in the control group (Fig 4, *B*). Massive IH was observed in the artery from the scramble group. Surprisingly, *CRE* decoy ODN treatment could morphologically prevent IH (Fig 4, *A*). When the pictures of the arteries were analyzed using the ImageJ image analysis software, *s*cramble decoy ODN treatment (wire treatment) had significantly increased the intima ratio and decreased the lumen and media ratio compared with the nonwire treatment (control; Fig 4, *C-E*). *CRE* decoy ODN treatment significantly increased the lumen ratio compared with the scramble decoy ODN (Fig 4, *C*). The intima and media ratios were significantly decreased by *CRE* decoy ODN treatment compared with those observed after treatment with the scramble decoy ODN (Fig 4, *D* and *E*). The adventitia ratio was not changed by either treatment (Fig 4, *F*).

These results suggest that *CRE* decoy ODN gene therapy can suppress IH formation in vivo.

MAPKAPK3 and FHL5 expression in human pregrafting vein remnants. Considering the possible future clinical application of *CRE* decoy ODN gene therapy, we needed to know who would require the treatment and which situations would be receptive to the treatment. Therefore, we investigated the expression of MAPKAPK3 and FHL5 in many human pregrafting vein remnants that were collected from patients with or without DM and maintenance HD, because MAPKAPK3 and FHL5 are the main activators of CREB in human vein wall IH situations. The samples were classified as good, fair, and poor vein quality for grafting by the intraoperative criteria described in a previous report.[30] In total, 27 samples were analyzed, including 9 non-DM and non-HD samples, 9 DM and non-HD samples, and 9 DM and HD samples, in which each group was further subdivided into 3 good, 3 fair, and 3 poor vein samples.

MAPKAPK3 expression of pregrafting vein remnants was significantly increased in the fair and poor vein remnants from the DM or non-HD patients (Fig 5, *A* and *B*). When the data were analyzed by the vein quality, MAPKAPK3 expression showed a tendency to be increased as the vein quality worsened (Fig 5, *C*). MAPKAPK3 expression was significantly increased in the samples from the DM and non-HD patients compared with that in the DM and HD patient samples when the data were analyzed by the patient background (Fig 5, *D*).

In contrast, FHL5 expression of pregrafting vein remnants in the non-DM and non-HD or DM and non-HD good vein remnants was significantly higher than in other remnants (Fig 6, *A* and *B*). When the data were analyzed by vein quality, FHL5 expression from the good vein remnants was significantly increased compared with that from the poor vein remnants (Fig 6, *C*). FHL5 expression was significantly decreased in the samples from the DM and HD patients compared with that observed in the DM and non-HD patient samples when the data were analyzed by patient background (Fig 6, *D*).

DISCUSSION

In this study, we confirmed and revealed that (1) a designed *CRE* decoy ODN can inhibit *CRE* activity via direct binding to activated CREB; (2) transfer of a *CRE* decoy ODN decreases VSMC proliferation and migration as well as (3) *Rac-1* and *Ccna2* expression in vitro; (4) *CRE* decoy ODN gene therapy can potently suppress the pathologic formation of IH, as well as *Bcl-2* and *Ccna2* expression in an animal model; (5) *MAPKAPK3* expression in pregrafting vein remnants is high in poor-quality and DM patient vein remnants; and (6) *FHL5* expression in pregrafting vein remnants is high in good-quality and DM patient vein remnants.

In general, transcription factor decoy ODNs, such as *CRE* decoy ODN are short, double-stranded DNA molecules[34] and are used as a novel class of nucleic acid-based drugs not only in vitro or in vivo but also in clinical applications.[9,35] Regarding its mode of action, after the transcription factor decoy ODN is taken into cells, the molecule can specifically bind to the relevant

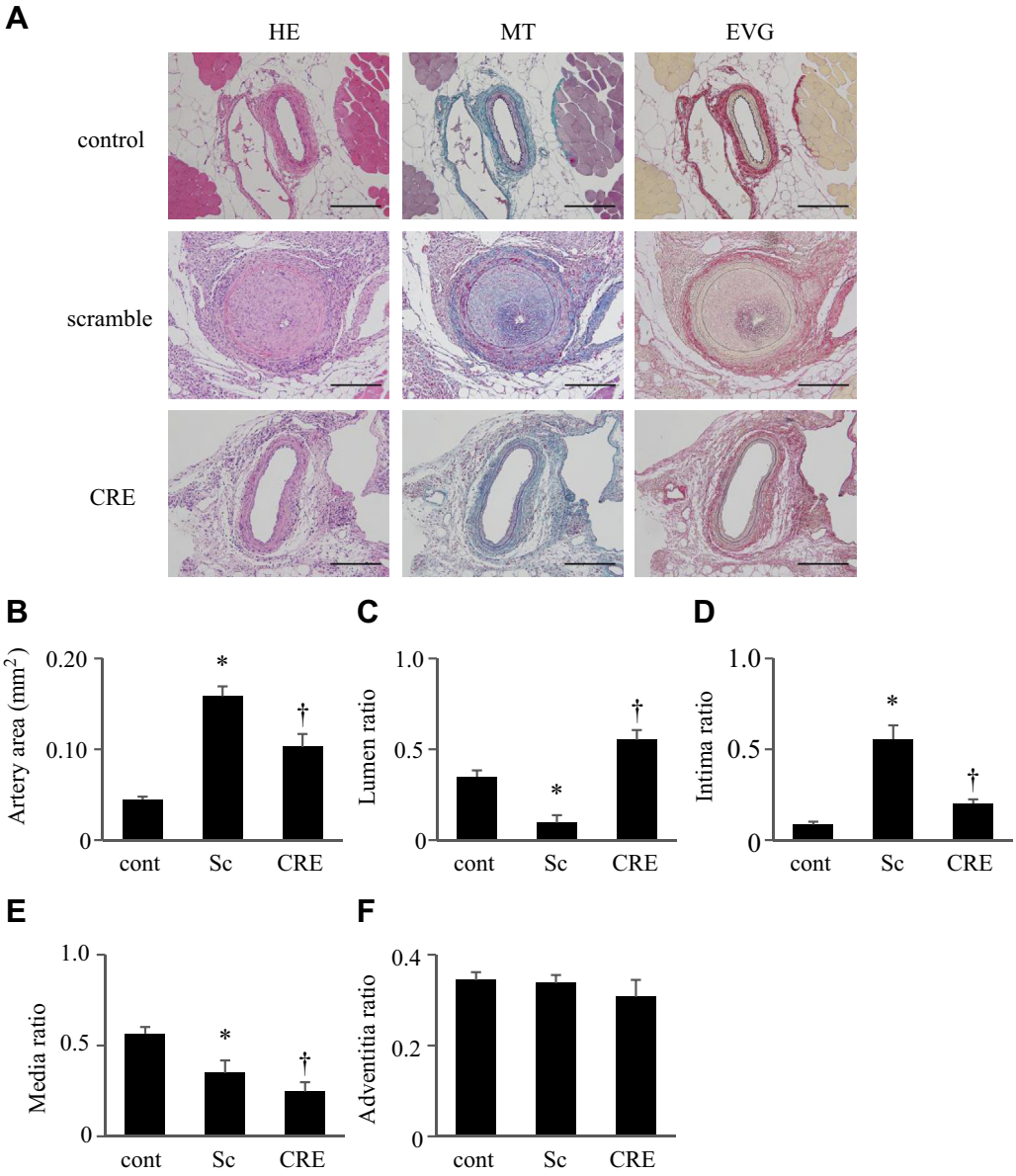

Fig 4. Gene therapy with cyclic adenosine monophosphate response element (*CRE*) decoy oligodeoxynucleotide (ODN) in vivo. **A,** Representative images of sham operation (control) arteries and scramble decoy ODN or *CRE* decoy ODN-transfected arteries stained with hematoxylin and eosin (*HE*), elastica Masson Trichrome (*MT*), and elastica van Gieson (*EVG*) at 21 days after vascular injury. *Bar* = 200 μm. Results of ImageJ image analysis of the vascular wall transfected with *CRE* decoy ODN or scramble (*Sc*) decoy *ODN* or subjected to sham operation only (*cont*) showing the **(B)** artery area, **(C)** lumen ratio, **(D)** intima ratio, **(E)** media ratio, and **(F)** adventitia ratio (n = 6). *$P < .05$ vs control. †$P < .05$ vs scramble decoy ODN.

transcription factor and interfere with the expression of several genes that are activated by the binding of the transcription factor to its *cis*-element. They do not necessarily block expression of the transcription factor itself. Our results showed that genes activated by *CRE*, such as *Bcl-2*, *Rac-1*, and *Ccna2*, were downregulated by transfer of the *CRE* decoy ODN, although *MAPKAPK3* and *FHL5* were not affected. These results are consistent with the proposed mode of action of transcription factor decoy therapy.

As shown in Fig 2, *FHL5* gene expression was not detected in the VSMC samples but was detected in the animal vein wall, as shown in Fig 3. It was difficult to verify the reason for this observation, but some speculations have been discussed. *Fhl5* is highly expressed in germ cells from male mice.[36] However, the human *FHL5* gene has not been detected in the adult testis, and the *FHL5* gene has only been found to be expressed in human tumor cell lines derived from squamous cell carcinoma, melanoma, and leukemia.[37] The VSMC

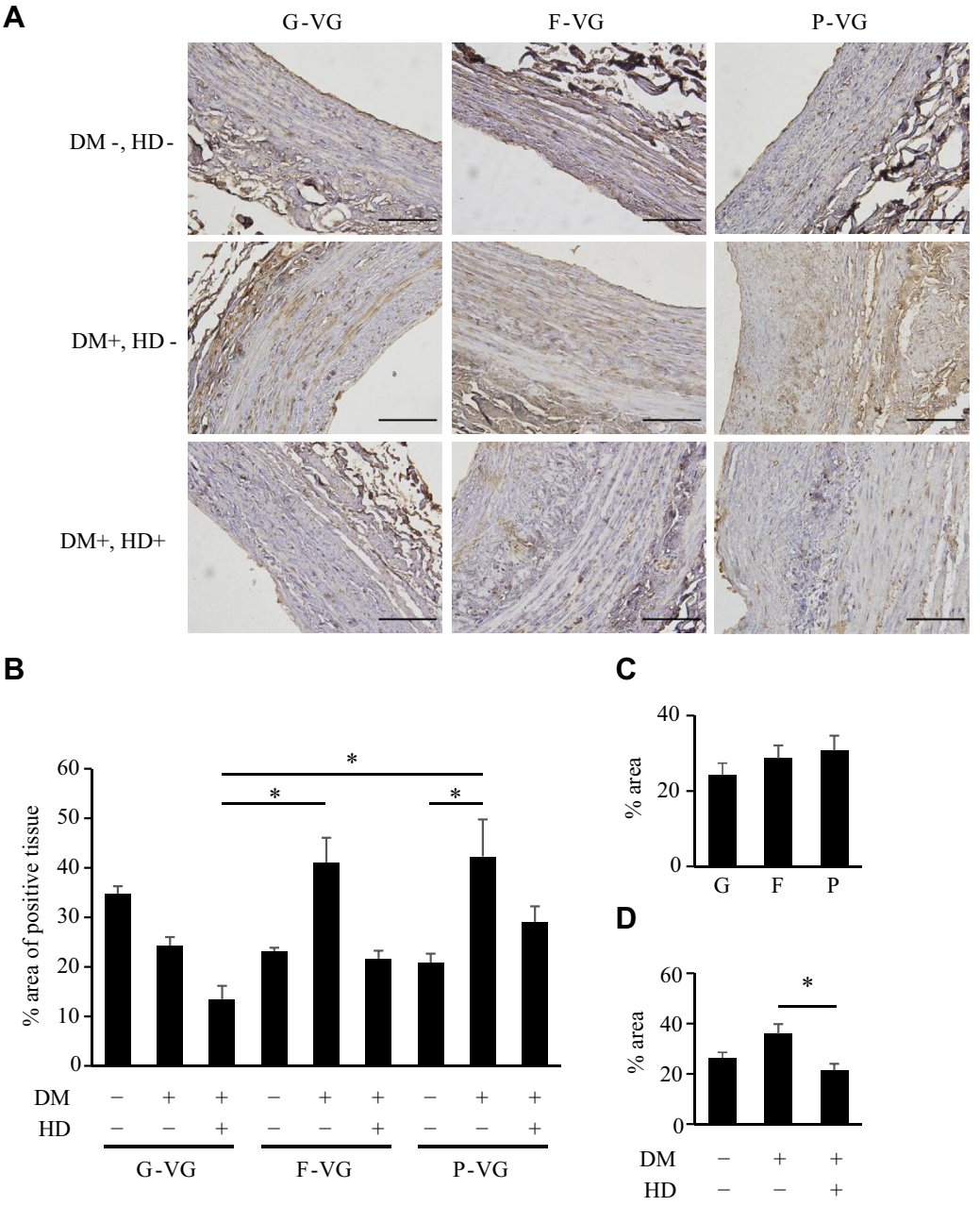

Fig 5. Mitogen-activated protein kinase-activated protein kinase 3 (MAPKAPK3) expression in human vein graft samples. **A,** Representative images of a human vein graft wall before transplantation and after MAPKAPK3 immunohistologic staining. *Bar* = 200 μm. Veins grafts (*VG*) are categorized as good-quality (*G-VG*), fair-quality (*F-VG*), and poor-quality (*P-VG*). **B,** Percentage area of MAPKAPK3-positive tissue analyzed by ImageJ software (n = 3). Subanalysis of images according to **(C)** good (*G*), fair (*F*) or poor (*P*) quality vein and **(D)** by diabetes mellitus (*DM*) and hemodialysis (HD) complication (n = 9) in each class. *$P < .05$.

phenotype changes from a contractile type to a synthetic-like type in response to change in gene expression.[38,39] Many VSMCs in the IH area showed synthetic-like type phenotypes. *FHL5* gene expression may depend on the VSMC phenotype, similar to that seen in carcinogenesis.

Our results showed that the *CRE* decoy ODN downregulated *Rac-1* expression in vitro but not in vivo. It also downregulated the expression of *Ccna-2* both in vitro and in vivo, but not *Fos*, although these genes are all downstream of the *CRE* element. We speculated that these discrepancies are caused by the complex mechanisms involved in the regulation of downstream genes of the *CRE* element, for instance, not only the *CRE* element but also alternative elements. Indeed, the promoter region of *FOS* has some *cis*-elements,

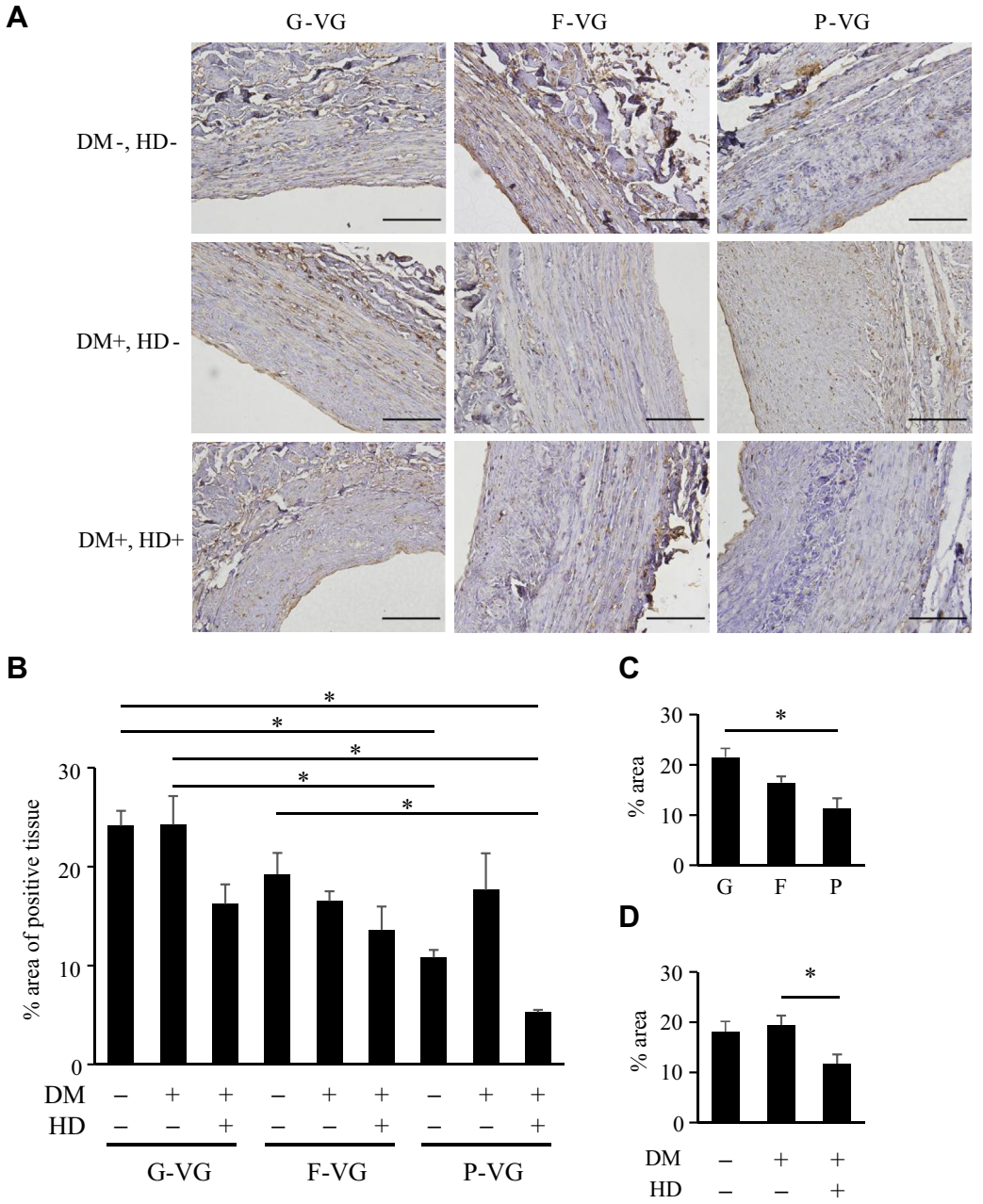

Fig 6. Expression of four and a half LIM domains 5 (FHL5) in human vein graft samples. **A,** Representative images of human vein graft walls before transplantation and after FHL5 immunohistologic staining. *Bar* = 200 μm. Vein grafts (*VG*) are classified as good-quality (*G-VG*), fair-quality (*F-VG*), and poor quality (*P-VG*). **B,** Percentage area of FHL5-positive tissue analyzed by ImageJ software (n = 3). Subanalysis of images according to **(C)** good-quality (*G*), fair-quality (*F*), or poor-quality (*P*) vein or **(D)** complication of diabetes mellitus (*DM*) and hemodialysis (*HD*), with n = 9 in each class. **P* < .05.

including *CRE*, serum response factor (*SRE*), and ternary complex factor (*TCF*).[40] These transcription factors are regulated by cell-to-cell signaling between endothelial cells, smooth muscle cells, fibroblasts, and circulating blood cells. In any case, the transfection of *CRE* decoy ODN could downregulate some *CRE* downstream genes, resulting in the suppression of IH formation.

Considering transcription factor decoy therapy, the sequence of *cis*-elements is conserved between species. Furthermore, the sequence can align with many binding sites in the promoter region of many target genes across different species.[41] Thus, the results from transcription factor decoy therapy experiments in animal models can be directly applied in initial clinical trials to assess safety and efficacy theoretically, although preclinical

studies must be conducted. According to previous studies of *E2F* and *NFKB*, there were no grave complications related to decoy transfer.[9,13]

Decoy delivery is an important issue for successful treatment. When the target of the decoy therapy was a vein for a graft, an *E2F* decoy using a nondistending pressure device resulted in the transfection of ~90% of the cells in the venous vessel wall.[42] In our study, the decoy was transfected using a microbubble-enhanced ultrasound method. Our decoy ODN transfection efficiency was >70%. We believe that a low-risk method is desirable for any strategy of gene transfer because PAD is a benign disease. If the decoy is used for endovascular therapy, a drug-eluting stent system, such as that used with the *NFKB* decoy ODN to prevent restenosis after percutaneous coronary intervention,[13] is helpful as a reference. A *CRE* decoy has already been used in humans as a tumor therapy and is considered to be a promising approach combined with radiotherapy.[43]

When *CRE* decoy therapy is performed on patients, the indications for its use are very important. The therapy cannot be used on all PAD or angina patients because of its high cost. Considering the indications for PAD patients treated with bypass surgery, vein quality for graft appears to be related to IH frequency. Good-quality veins rarely induce IH, but poor-quality veins have a high risk of IH and graft failure.[33,44] However, considerations about *CRE* decoy therapy could not indicate vein quality in our study, because MAPKAPK3 expression was higher in poor-quality veins than in good-quality veins, whereas FHL5 expression was lower in poor-quality veins. Thus, *CRE* was activated regardless of vein quality. In contrast, MAPKAPK3 and FHL5 were both highly expressed in DM patients. Given these results, the priority for *CRE* decoy therapy may be DM patients with whole vein quality. It was unexpected that MAPKAPK3 and FHL5 were not upregulated or downregulated in HD patients. Thus, further study of this issue is required.

CONCLUSIONS

We revealed that CREB-CRE signaling is an important mechanism in IH formation and that *CRE* decoy therapy can help to prevent IH. Furthermore, we suggest that DM patients are a good match for this treatment based on immunohistologic analysis. This study is part of the preclinical study of our strategy, which will be followed by the pharmacologic (including the verification of mode of action), pharmacokinetic, and safety studies. We believe that the results from our present study will provide a new approach for controlling IH after vascular and endovascular surgery.

We thank Dr Hisashi Uchida, Associate Professor Atsuhiro Koya, and former Associate Professor Masashi Inaba, Department of Surgery, Asahikawa Medical University for providing the human vein remnants as samples.

AUTHOR CONTRIBUTIONS

Conception and design: YS, TS
Analysis and interpretation: DU, YS
Data collection: DU, SK, YY, SH, TS, NA
Writing the article: DU, YS, SK, YY, SH, TS, NA
Critical revision of the article: DU, YS, TS
Final approval of the article: DU, YS, SK, YY, SH, TS, NA
Statistical analysis: DU, YS
Obtained funding: YS
Overall responsibility: YS

REFERENCES

1. Lal BK, Beach KW, Roubin GS, Lutsep HL, Moore WS, Malas MB, et al. Restenosis after carotid artery stenting and endarterectomy: a secondary analysis of CREST, a randomised controlled trial. Lancet Neurol 2012;11:755-63.
2. Taylor LM Jr, Edwards JM, Porter JM. Present status of reversed vein bypass grafting: five-year results of a modern series. J Vasc Surg 1990;11:193-205.
3. Conte MS, Belkin M, Upchurch GR, Mannick JA, Whittemore AD. Impact of increasing comorbidity on infrainguinal reconstruction: a 20-year perspective. Ann Surg 2001;233:445-52.
4. Mills J. Infrainguinal bypass. In: In: Rutherford R, editor. Vascular surgery. 6th ed., Vol 1. Philadelphia: Elsevier Saunders; 2005. p. 1154-74.
5. Dember LM, Beck GJ, Allon M, Delmez JA, Dixon BS, Greenberg A, et al. Effect of clopidogrel on early failure of arteriovenous fistulas for hemodialysis: a randomized controlled trial. JAMA 2008;299:2164-71.
6. Muto A, Model L, Ziegler K, Eghbalieh SD, Dardik A. Mechanisms of vein graft adaptation to the arterial circulation: insights into the neointimal algorithm and management strategies. Circ J 2010;74:1501-12.
7. Morice MC, Serruys PW, Barragan P, Bode C, Van Es GA, Stoll HP, et al. Long-term clinical outcomes with sirolimus-eluting coronary stents: five-year results of the RAVEL trial. J Am Coll Cardiol 2007;50:1299-304.
8. Greenhalgh J, Hockenhull J, Rao N, Dundar Y, Dickson RC, Bagust A. Drug-eluting stents versus bare metal stents for angina or acute coronary syndromes. Cochrane Database Syst Rev 2010:CD004587.
9. Conte MS, Bandyk DF, Clowes AW, Moneta GL, Seely L, Lorenz TJ, et al. Results of PREVENT III: a multicenter, randomized trial of edifoligide for the prevention of vein graft failure in lower extremity bypass surgery. J Vasc Surg 2006;43:742-51; discussion: 751.
10. Alexander JH, Hafley G, Harrington RA, Peterson ED, Ferguson TB Jr, Lorenz TJ, et al. Efficacy and safety of edifoligide, an E2F transcription factor decoy, for prevention of vein graft failure following coronary artery bypass graft surgery: PREVENT IV: a randomized controlled trial. JAMA 2005;294:2446-54.
11. Mitra AK, Gangahar DM, Agrawal DK. Cellular, molecular and immunological mechanisms in the pathophysiology of vein graft intimal hyperplasia. Immunol Cell Biol 2006;84:115-24.
12. Miyake T, Aoki M, Shiraya S, Tanemoto K, Ogihara T, Kaneda Y, et al. Inhibitory effects of NFkappaB decoy oligodeoxynucleotides on neointimal hyperplasia in a rabbit vein graft model. J Mol Cell Cardiol 2006;41:431-40.
13. Egashira K, Suzuki J, Ito H, Aoki M, Isobe M, Morishita R. Long-term follow up of initial clinical cases with NF-kappaB

decoy oligodeoxynucleotide transfection at the site of coronary stenting. J Gene Med 2008;10:805-9.
14. Puhakka HL, Turunen P, Gruchala M, Bursill C, Heikura T, Vajanto I, et al. Effects of vaccinia virus anti-inflammatory protein 35K and TIMP-1 gene transfers on vein graft stenosis in rabbits. In Vivo (Brooklyn) 2005;19:515-21.
15. Eefting D, de Vries MR, Grimbergen JM, Karper JC, van Bockel JH, Quax PH. In vivo suppression of vein graft disease by nonviral, electroporation-mediated, gene transfer of tissue inhibitor of metalloproteinase-1 linked to the amino terminal fragment of urokinase (TIMP-1.ATF), a cell-surface directed matrix metalloproteinase inhibitor. J Vasc Surg 2010;51:429-37.
16. Hu Y, Baker AH, Zou Y, Newby AC, Xu Q. Local gene transfer of tissue inhibitor of metalloproteinase-2 influences vein graft remodeling in a mouse model. Arter Thromb Vasc Biol 2001;21:1275-80.
17. Kallenbach K, Salcher R, Heim A, Karck M, Mignatti P, Haverich A. Inhibition of smooth muscle cell migration and neointima formation in vein grafts by overexpression of matrix metalloproteinase-3. J Vasc Surg 2009;49:750-8.
18. Wolff RA, Malinowski RL, Heaton NS, Hullett DA, Hoch JR. Transforming growth factor-beta1 antisense treatment of rat vein grafts reduces the accumulation of collagen and increases the accumulation of h-caldesmon. J Vasc Surg 2006;43:1028-36.
19. Kloppenburg GT, Grauls GE, Bruggeman CA, Stassen FR. Adenoviral activin A expression prevents vein graft intimal hyperplasia in a rat model. Interact Cardiovasc Thorac Surg 2009;8:31-4.
20. de Graaf R, Tintu A, Stassen F, Kloppenburg G, Bruggeman C, Rouwet E. N-acetylcysteine prevents neointima formation in experimental venous bypass grafts. Br J Surg 2009;96:941-50.
21. Luo Z, Asahara T, Tsurumi Y, Isner JM, Symes JF. Reduction of vein graft intimal hyperplasia and preservation of endothelium-dependent relaxation by topical vascular endothelial growth factor. J Vasc Surg 1998;27:167-73.
22. Wan S, George SJ, Nicklin SA, Yim AP, Baker AH. Overexpression of p53 increases lumen size and blocks neointima formation in porcine interposition vein grafts. Mol Ther 2004;9:689-98.
23. Mayr U, Mayr M, Li C, Wernig F, Dietrich H, Hu Y, et al. Loss of p53 accelerates neointimal lesions of vein bypass grafts in mice. Circ Res 2002;90:197-204.
24. Kusch B, Waldhans S, Sattler A, Wagner A, Hecker M, Moosdorf R, et al. Inhibition of carotis venous bypass graft disease by intraoperative nucleic acid-based therapy in rabbits. Thorac Cardiovasc Surg 2006;54:388-92.
25. Nakanishi K, Saito Y, Azuma N, Sasajima T. Cyclic adenosine monophosphate response-element binding protein activation by mitogen-activated protein kinase-activated protein kinase 3 and four-and-a-half LIM domains 5 plays a key role for vein graft intimal hyperplasia. J Vasc Surg 2013;57:182.e1-10.
26. Sun L, Zhao R, Zhang L, Zhang W, He GR, Yang S, et al. Prevention of vascular smooth muscle cell proliferation and injury-induced neointimal hyperplasia by CREB-mediated p21 induction: an insight from a plant polyphenol. Biochem Pharmacol 2016;103:40-52.
27. Tokunou T, Shibata R, Kai H, Ichiki T, Morisaki T, Fukuyama K, et al. Apoptosis induced by inhibition of cyclic AMP response element-binding protein in vascular smooth muscle cells. Circulation 2003;108:1246-52.
28. Abizaid A, Kornowski R, Mintz GS, Hong MK, Abizaid AS, Mehran R, et al. The influence of diabetes mellitus on acute and late clinical outcomes following coronary stent implantation. J Am Coll Cardiol 1998;32:584-9.
29. Wang P, Huang S, Wang F, Ren Y, Hehir M, Wang X, et al. Cyclic AMP-response element regulated cell cycle arrests in cancer cells. PLoS One 2013;8:2-8.
30. Park YG, Nesterova M, Agrawal S, Cho-Chung YS. Dual blockade of cyclic AMP response element-(CRE) and AP-1-directed transcription by CRE-transcription factor decoy oligonucleotide: gene-specific inhibition of tumor growth. J Biol Chem 1999;274:1573-80.
31. Park YG, Park S, Lim SO, Lee MS, Ryu CK, Kim I, et al. Reduction in cyclin D1/Cdk4/retinoblastoma protein signaling by CRE-decoy oligonucleotide. Biochem Biophys Res Commun 2001;281:1213-9.
32. Sata M, Maejima Y, Adachi F, Fukino K, Saiura A, Sugiura S, et al. A mouse model of vascular injury that induces rapid onset of medial cell apoptosis followed by reproducible neointimal hyperplasia. J Mol Cell Cardiol 2000;32:2097-104.
33. Sasajima T, Kubo Y, Kokubo M, Izumi Y, Inaba M. Comparison of reversed and in situ saphenous vein grafts for infragenicular bypass: experience of two surgeons. Cardiovasc Surg 1993;1:38-43.
34. Morishita R, Gibbons GH, Horiuchi M, Ellison KE, Nakama M, Zhang L, et al. A gene therapy strategy using a transcription factor decoy of the E2F binding site inhibits smooth muscle proliferation in vivo. Proc Natl Acad Sci U S A 1995;92:5855-9.
35. Sen M, Thomas SM, Kim S, Yeh JI, Ferris RL, Johnson JT, et al. First-in-human trial of a STAT3 decoy oligonucleotide in head and neck tumors: implications for cancer therapy. Cancer Discov 2012;2:694-705.
36. Fimia GM, De Cesare D, Sassone-Corsi P. CBP-independent activation of CREM and CREB by the LIM-only protein ACT. Nature 1999;398:165-9.
37. Morgan MJ, Whawell SA. The structure of the human LIM protein ACT gene and its expression in tumor cell lines. Biochem Biophys Res Commun 2000;273:776-83.
38. Yoshiyama S, Chen Z, Okagaki T, Kohama K, Nasu-Kawaharada R, Izumi T, et al. Nicotine exposure alters human vascular smooth muscle cell phenotype from a contractile to a synthetic type. Atherosclerosis 2014;237:464-70.
39. Vilamaior PS, Taboga SR, Carvalho HF. Modulation of smooth muscle cell function: morphological evidence for a contractile to synthetic transition in the rat ventral prostate after castration. Cell Biol Int 2005;29:809-16.
40. Janknecht R. Regulation of the c-fos promoter. Immunobiology 1995;193:137-42.
41. Mann MJ. Transcription factor decoys: a new model for disease intervention. Ann N Y Acad Sci 2005;1058:128-9.
42. Ehsan A, Mann MJ, Dell'Acqua G, Dzau VJ. Long-term stabilization of vein graft wall architecture and prolonged resistance to experimental atherosclerosis after E2F decoy oligonucleotide gene therapy. J Thorac Cardiovasc Surg 2001;121:714-22.
43. Park SI, Park SJ, Lee J, Kim HE, Park SJ, Sohn JW, et al. Inhibition of cyclic AMP response element-directed transcription by decoy oligonucleotides enhances tumor-specific radiosensitivity. Biochem Biophys Res Commun 2016;469:363-9.
44. Bradbury AW, Adam DJ, Bell J, Forbes JF, Fowkes FG, Gillespie I, et al. Bypass versus Angioplasty in Severe Ischaemia of the Leg (BASIL) trial: analysis of amputation free and overall survival by treatment received. J Vasc Surg 2010;51:18S-31S.

Submitted Aug 14, 2018; accepted Feb 17, 2019.